Ultramicroscopy 193 (2018) 126–136

Contents lists available at ScienceDirect

Ultramicroscopy

journal homepage: www.elsevier.com/locate/ultramic

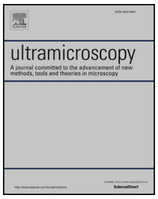

Resolution of transmission electron backscatter diffraction in aluminum and silver: Effect of the atomic number

Chia-Wei Kuo[a], Jui-Chao Kuo[a,*], Sheng-Chang Wang[b]

[a] Department of Materials Science and Engineering, National Cheng Kung University, Tainan 701, Taiwan, ROC
[b] Department of Mechanical Engineering, Southern Taiwan University of Technology, Tainan 71005, Taiwan, ROC

ARTICLE INFO

Keywords:
Atomic number
t-EBSD
Spatial resolution
Depth resolution
Aluminum
Silver

ABSTRACT

This work aims to investigate the influence of intrinsic and extrinsic factors on the physical resolution of the transmission electron backscattered diffraction technique (t-EBSD) in aluminum and silver. Here, we focus on the intrinsic factors, namely, atomic number and thickness of the specimen, and extrinsic set-up factors, which include the electron beam voltage, working distance, and specimen tilt. The working distance and tilt angle, which are selected as 12 mm and 60° for Al and 12 mm and 50° for Ag, respectively, reveal a sharp pattern with high contrast. The physical resolutions at the lateral and longitudinal directions depend on the depth resolution. The depth and lateral and longitudinal resolutions increase in Al but decrease in Ag with increased accelerating voltage. The decrease in specimen thickness for Al and Ag from 400 nm to 100 nm reduces the lateral and longitudinal resolutions. The most ideal depth and lateral and longitudinal resolutions obtained under a thickness of 100 nm are 22.7, 18.9, and 33.7 nm at 30 kV for Ag and 34.7, 22.8, and 36.6 nm at 15 kV for Al, respectively.

1. Introduction

Electron backscatter diffraction (EBSD) has been widely applied to analyze material microstructures [1,2] with grain sizes ranging from centimeters to submicrons. The spatial resolution of EBSD is influenced with various factors, such as the backscattering coefficient, electron beam spot size [3,4], excitation volume [2,5,6], and pattern-indexing software [5,7]. Several methods, such as reducing the accelerating voltage [5], incorporating an energy filter [8], and decreasing the specimen thickness [9,10], have been proposed to improve the spatial resolution of EBSD. Hence, spatial resolution depends not only on intrinsic factors, such as density, atomic number (*Z*), and specimen thickness, but also on extrinsic factors, such as accelerating voltage, specimen tilt, and detector position.

Geiss et al. [10] demonstrated Kikuchi diffraction through scanning electron microscopy (SEM) in transmission mode to improve the spatial resolution of a transmission electron microscopic specimen to the nanoscale in a process called transmission EBSD (t-EBSD). Such a specimen is tilted to α of − 20° relative to the incident beam, that is, in a direction opposite that in an EBSD mode to prevent the shadowing effects and backscattered electrons from reaching the charge-coupled device camera [10,12]. Keller and Geiss [13] presented the Kikuchi patterns of t-EBSD from Fe–Co nanoparticles with a diameter of 10 nm and from an in-plane grain size of 15 nm in 40 nm-thick Ni films. Trimby [14] showed that the spatial resolutions of t-EBSD are 5–10 and 10 nm in electrodeposited nanocrystalline Ni and Al alloys, respectively. Brodusch et al. [11] indexed the Kikuchi diffraction patterns of Pd nanoparticles with a size of 5.6 nm. Birosca et al. [15] and Suzuki [16] detected small $Cr_{23}C_6$ precipitates of approximately 30 nm in Cr–Mo–V steel.

In SEM, EBSD is used for orientation mapping and phase identification at a minimum spatial resolution of several tens of nanometers, depending on the average *Z* of a sample [2]. In transmitted Kikuchi diffraction, the quality of diffraction patterns depends on the *Z* and material density, sample thickness, microstructure, plastic strain, and SEM conditions [15]. Table 1 summarizes the spatial resolution of t-EBSD in terms of accelerating voltage, working distance, and tilt angle. The spatial resolution of t-EBSD is indirectly related to *Z*.

In the current study, we initially investigated the factors of working distance and specimen tilt on the quality of Kikuchi patterns and subsequently studied the effects of accelerating voltage and specimen thickness on the physical resolution of t-EBSD in aluminum ($Z = 13$) and silver ($Z = 47$), respectively. Here physical resolution means the depth and spatial resolutions along the longitudinal and lateral directions.

---

[*] Corresponding author.
E-mail address: jckuo@mail.ncku.edu.tw (J.-C. Kuo).

https://doi.org/10.1016/j.ultramic.2018.06.019
Received 26 May 2018; Received in revised form 21 June 2018; Accepted 27 June 2018

Table 1

Summary of the spatial resolution of transmission electron backscattered diffraction (t-EBSD).

Metals	Z	d (nm)	K (kV)	D (mm)	θ (°)	Ref.
Al	13	10	30	6	0	[14]
Al	13	5	30	6	−20	[11]
$Cr_{23}C_6$		30	20	5	−40	[16]
Steel	26	5–10	20	7.5	−12	[15]
Steel	26	7^+	30	2	−20	[29]
Ni	28	2	30	6	0	[14]
Cu	29	10	30	5–7	−20	[13]
Cu	29	25.2^+	30	12	−20	[24]

Note: + is absolute spatial resolution. Z is the atomic number, d the resolution, K the accelerating voltage, D the working distance, θ the tilt angle.

2. Materials and experiments

2.1. Material and sample preparation

First, the effects of working distance and tilt angle on the quality of Kikuchi patterns obtained from t-EBSD were investigated by using a single-crystal specimen named specimen A. Afterward, bicrystals with tilted grain boundaries termed specimen C were used to determine the physical resolution of depth. Finally, bicrystals with planar grain boundaries labeled specimen B were utilized to measure the physical resolutions along the longitudinal and lateral directions. To produce specimens A, B, and C from polycrystalline Ag and Al, we annealed 99.999% pure Ag and Al for 24 h at 900 °C and 600 °C, respectively. The specimens were ground and polished with diamond suspensions and subsequently submerged in an etching solution, which contained NaOH (2 g), Na_2CO_3 (4 g), and DI water (94 mL) for Al for 20–25 min. Afterward, the specimens were placed in an etching solution that contained CH_3OH (40 mL), H_2O_2 (10 mL), and NH_4OH (10 mL) for Ag for 30–40 s. Etching revealed the grain boundary of bicrystals, which enabled the selection of defined bicrystals and cutting of specimens through focus ion beam (FIB) milling.

FIB milling was conducted to cut the specimens into 8 μm × 10 μm dimensions with defined thickness in the range of 100–400 nm under a gallium ion beam at 5 kV. After cutting the specimens, their defined thicknesses were directly examined by observing the FIB images; 200, 100, and 100–400 nm thicknesses were obtained for specimens A, C, and B, respectively.. With regard to coarse and fine polishing, the beam currents of 2 nA and 25 pA were applied to reduce layer damage at the top and bottom surfaces, respectively, of the specimens. Afterward, all of the t-EBSD specimens were welded and fixed in a Cu ring.

2.2. t-EBSD measurements

When the samples were prepared, t-EBSD measurements were performed using a JEOL 7001F field emission SEM equipped with EDAX/TSL data collection software, together with a homemade sample holder. The resolution of the DigiView camera was 1392 × 1024 pixels, and the exposure time was 0.5 s. The t-EBSD experiments were conducted five times for each testing condition. Here, the working distance was at 12–15 mm, and the tilt angle was 10°–60° for specimen A with 200 nm thickness at 25 kV to obtain sharp Kikuchi patterns with high contrast. The t-EBSD setup is schematically illustrated in Fig. 1. The normal angle of the specimen was tilted to the angle called the tilt angle.

To investigate the depth resolution of specimen C, we recorded the Kikuchi patterns of t-EBSD at accelerating voltages of 15–30 kV with 5 kV increments at a scanning step of 2 nm across the boundary. The boundary was perpendicular and parallel to the rotation axis of SEM to determine the respective lateral and longitudinal resolutions for specimen B at varying thicknesses of 100–400 nm.

3. Results and discussion

3.1. Effects of working distance and tilt angle on the pattern quality

Figs. 2 and 3 show the Kikuchi patterns of Al and Ag with a 200 nm thickness at 25 kV, respectively. In order to avoid taking the areas out of the circular image containing diffraction patterns into accounting, we just used the same rectangular maximum area inside the circular image obtained from the circular phosphor. We adapted two quantitative methods to identify their contrast and sharpness and detect the quality of Kikuchi patterns. A contrast metric called Michelson contrast [17] was defined as follows:

$$C = \frac{C_{\max} - C_{\min}}{C_{\max} + C_{\min}}, \tag{1}$$

where $C_{\min}$ and $C_{\max}$ denote the minimum and maximum values of grayscale, respectively.

Krieger Lassen et al. [18] proposed that the inertia I of Fourier spectrum should be normalized to the total energy of Fourier spectrum through fast Fourier transform. A poor-quality pattern holds a more homogenous spectrum than that of a high-quality pattern. This observation means that a sharp pattern consists of a large part of the low frequencies, whereas a worse pattern exhibits a frequency spectrum of white noise. The measurement of the uniformity of the frequency spectrum is called the inertia I of the Fourier spectrum. Inertia I is defined as follows:

$$I = \frac{\sum_{i,j} (i-j)^2 P(i,j)}{\sum_{i,j} P^2(i,j)}, \tag{2}$$

where $P(i, j)$ is the grayscale at each position of i and j. In Fig. 4, the highest C was observed at the tilt angle of 60°, and C increased when the working distance decreased from 15 mm to 12 mm for Al. The lowest inertia was obtained at a working distance of 13 mm and a tilt angle of 60° Thus, the working distance of 13 mm and the tilt angle of 60° were selected as operating parameters for subsequent studies involving Al; the working distance and tilt angle for Ag were 12 nm and 50°, respectively (Figs. 5(a) and 5(b)). In this work, the shortest working distance was limited by 12 mm because of the collision between SEM and the sample holder. We found that the contrast of Kikuchi patterns increases with the increased tilt angle. This observation corresponded to the results shown in Figs. 2 and 3.

The operating parameters of the working distance and tilt angle for t-EBSD from previous studies are summarized as follows. Keller and Geiss [13] reported that a strong signal occurs at tilt angles of 10°–30° under accelerating voltages in the range of 15–30 kV with a working distance of 3–12 mm using LEO 1525 field-emission SEM. Suzuki [16] suggested the tilt angle range of 30°–40° and the working distance in the range of 4–5 mm achieved using JEOL JSM-7001F SEM. Trimby [14] applied the tilt angle of 20° and the working distance of 5 mm by using Zeiss Ultra Plus FEG SEM. Brodusch et al. [19] presented that the tilt angle in the range of 20°–40° is suitable for obtaining good-quality Kikuchi pattern through Hitachi SU 8000. Working distance was selected between 11 mm and 16 mm to reduce the influence of the magnetic field and avoid shadowing on the pattern image. Furthermore, large tilt angles result in enlarged spatial resolution in STEM images because of the increased interaction volume at a high tilt angle [19]. Hence, the operating parameters of the working distance and tilt angle for t-EBSD strongly depend on each operation system of SEM and EBSD. To understand the influences of working distance and tilt angle, the formation of Kikuchi patterns was briefly discussed in Section 3.2 of effects of accelerating voltage and Z on depth resolution.

The simplified electron transport properties are schematically shown in Fig. 6 for the tilt angles of 30° and 60° With consideration of the case of 60° in Fig. 6(b), the shortest incoming and outgoing path lengths of electrons correspond to L_p and L_d, respectively. The shortest